

## OBSERVATIONS OF CLOUD AND AEROSOL FROM GCOM-C SGLI

T. Y. Nakajima<sup>a,\*</sup>, M. Kuji<sup>b</sup>, I. Sano<sup>c</sup>, Nick Schutgens<sup>d</sup>, Y. Mano<sup>e</sup>, J. Riedi<sup>f</sup>,  
H. Ishida<sup>g</sup>, K. Suzuki<sup>h</sup>, H. Okamoto<sup>i</sup>, T. Matsui<sup>a</sup>, H. Letu<sup>a</sup>

<sup>a</sup> TRIC, Tokai University, 151-0063, Tokyo, Japan - nkjm@yoyogi.ycc.u-tokai.ac.jp

<sup>b</sup> Nara Women's University 630-8506, Nara, Japan - makato@ics.nara-wu.ac.jp

<sup>c</sup> Kinki University, 577-8502, Osaka, Japan - sano@info.kindai.ac.jp

<sup>d</sup> AORI, The University of Tokyo, 277-8568, Kashiwa, Chiba, Japan - schutgen@aori.u-tokyo.ac.jp

<sup>e</sup> Meteorological Research Institute, 305-0052, Tsukuba, Ibaraki, Japan - ymano@mri-jma.go.jp

<sup>f</sup> Universite de Lille 1, France, - riedi@loa630.univ-lille1.fr

<sup>g</sup> Yamaguchi University, Ube, Yamaguchi, Japan, - ishidah@yamaguchi-u.ac.jp

<sup>h</sup> Colorado State University, 80523-1371, Ft. Collins, CO, USA - kenta@atmos.colostate.edu

<sup>i</sup> RIAM, Kyushu University, 816-8580 - okamoto@riam.kyushu-u.ac.jp

### Commission VIII

**KEY WORDS:** GCOM, SGLI, Cloud, Aerosol, ADEOS-II, GLI, Assimilation, Cloud Radar, EarthCARE

### ABSTRACT:

Observing cloud and aerosol distributions and their optical and microphysical properties are one of important activities for the global climate change study, since the role of these particles and their interactive responses to the climate system are still in mystery. The Second generation Global Imager (SGLI) aboard the GCOM-C satellite is a follow-on sensor of the Global Imager (GLI) aboard the Midori-2 satellite. It is designed for globally observing clouds and aerosols targets with high-accuracy and quick recurrence. The major geophysical parameters retrieved from SGLI atmosphere's algorithm are cloud optical thickness, cloud particle radii, cloud top temperature, cloud geometrical thickness, aerosol optical thickness, and aerosol Angstrom exponents. Cloud discriminations all of SGLI pixels will also be supplied. It is notable that the SGLI has some functions specialized for observing aerosol properties over ocean and land. They are 0.38- $\mu\text{m}$  channels, multi-angles and polarization capability in 0.67 and 0.86- $\mu\text{m}$  channels. This paper introduces strategy of the atmospheric observations by use of the GCOM-C/SGLI and the latest research results obtained from GLI-to-SGLI scientific activities.

## 1. INTRODUCTION

### 1.1 Importance of cloud and aerosol observations

Clouds and aerosols are important observation targets in the atmosphere for understanding the mechanisms of climate and for predicting climate changes. The International Panel on Climate Change (IPCC) Forth Assessment Report (AR4) (Solomon, 2007) pointed out that the clouds are still characterized by large uncertainties in the estimation of their effects on energy balance of the Earth's atmosphere. From this point of view, it is important to reveal the process of the growth of cloud droplets and their interactions with aerosols, as well as the global distribution of clouds and their microphysical properties. The importance of any factor directly and/or indirectly affecting the energy balance is expressed in terms of "radiative forcing", which is used for understanding how a range of human and natural factors contribute to the warming or cooling of the global climate. Radiative forcing is defined as the difference in energy balance between the pre-industrial and present epochs. Positive and negative values of radiative forcing indicate warming and cooling, respectively. For example, AR4 has reported that carbon dioxide, which is a greenhouse gas, has a radiative forcing value of +1.66  $\text{W/m}^2$  (warming), whereas the change of the cloud albedo associated with the change of the aerosol concentration in the atmosphere is -0.7  $\text{W/m}^2$  (cooling). This suggests that the warming effects of e.g. carbon dioxide are canceled in part by the cooling effects of clouds through changes in the aerosol concentration. However, the estimated

radiative forcing due to the cloud albedo effect is still associated with large uncertainties regarding its value, which varies in the range of -1.8 to -0.3  $\text{W/m}^2$ . This uncertainty is mainly due to insufficient knowledge regarding aerosol-cloud interactions. Therefore, global-scale observations of clouds and aerosols, as well as the modeling of cloud-aerosol interactions, are important research activities in climate studies.

### 1.2 Heritages of the Midori-II GLI and new sights

The Midori-II Global Imager (GLI) mission was one of our successes. We will use the heritage of the GLI science mission to the SGLI mission. At the same time, we challenge cloud and aerosol observations with new sights of the science. The cloud-screening algorithm developed by S. Ackerman (1998) was installed as the Midori-II GLI standard algorithm. We have been developing, individually, a new cloud screening algorithm referring the Ackerman's algorithm (the heritage of the GLI mission), but gave drastically re-construct the structure of the algorithm. The concept of a clear confidence level (= Q value), which represents certainty of the clear or cloud condition, is applied to design a neutral cloud detection algorithm that is not biased to either clear or cloudy. The use of the clear Q value with neutral concept also makes our algorithm structure very simple. This algorithm is the Cloud and Aerosol Unbiased Decision Intellectual Algorithm (CLAUDIA) developed by Ishida and Nakajima (2009).

The former version of the Comprehensive Analysis Program for Cloud Optical Measurements (CAPCOM) has been installed

\* Corresponding author. [http://www.yc.ycc.u-tokai.ac.jp/ns/nakajimlab/top\\_e.html](http://www.yc.ycc.u-tokai.ac.jp/ns/nakajimlab/top_e.html)

Table 1 Channel specification of the SGLI (appeared in RA2 document by JAXA)

SGLI OBSERVATION REQUIREMENT DETAILS						
	CH	$\lambda$	$\Delta\lambda$	IFOV	SNR	L (for SNR)
		nm: VNR, IRS SWI $\mu\text{m}$ : IRS TIR	m		SNR: VNR, IRS SWI NEAT(K): IRS TIR	
VNR-NP	VN1	380	10	250	250	60
	VN2	412	10	250	400	75
	VN3	443	10	250	300	64
	VN4	490	10	250	400	53
	VN5	530	20	250	250	41
	VN6	565	20	250	400	33
	VN7	670	10	250	400	23
	VN8	670	20	250	250	25
	VN9	763	8	1000	400	40
	VN10	865	20	250	400	8
	VN11	865	20	250	200	30
VNR-P	P1	670	20	1000	250	25
	P2	865	20	1000	250	30
IRS SWI	SW1	1050	20	1000	500	57
	SW2	1380	20	1000	150	8
	SW3	1630(TBD)	200	250	57	3
	SW4	2210	50	1000	211	1.9
IRS TIR	T1	10.8	0.7	500	0.2	300 (K)
	T2	12.0	0.7	500	0.2	300 (K)

in the Midori-II/GLI data analysis system in JAXA (named ATSK3R) and used for retrieving the cloud microphysical properties, as the Midori-II GLI standard algorithm. The system was successfully operated and yielded 7-month archives of the global cloud properties. The algorithm development strategy of the Midori-II GLI atmosphere mission is summarized in Nakajima et al. (2009a). We have been improving the CAPCOM algorithm with sights of the new perspective in the SGLI era mentioned in the next subsection. Both the GLI and SGLI equip 0.763- $\mu\text{m}$  oxygen-A band. This is used for retrieving cloud geometrical thickness together with some additional properties such as cloud optical thickness, cloud top heights. We are going to improve research algorithms developed during GLI-era. Some algorithm extensions towards ice cloud retrievals are also our targets in the SGLI. For this aim, we have been developing some scattering solvers based on geometrical optics approximations (GOA) and boundary elements method that calculate light scattering of small particles (Nakajima et al. 1997, Mano 2000, Nakajima et al. 2009b).

Aerosol retrievals had been performed by ATSK5 as the GLI standard product that uses 2-channels from in the GLI (Higurashi et al. 2000). In the SGLI-era, we are proposing multi-information method that will use two polarization channels, multi-angle, un-polarized near-ultra violet channel and visible channel of the SGLI for retrieving aerosol optical thickness, size information, and aerosol absorptivity.

### 1.3 SGLI band specifications

The Second generation GLobal Imager (SGLI) is the passive imager that has 19 observing channels from near ultra violet (NUV) to thermal infrared (TIR). Most of NUV to TIR channels have 250m Instantaneous Field Of View (IFOV) except for Oxygen-A bands in 763nm channel (1000m). The SGLI equipped two polarization / changeable angel (0, 60, and 120 degrees) channels in 670nm and 865nm. These polarization channels are designed for mainly observations of atmospheric aerosols. In the shortwave infrared region, the SGLI has four channels in 1050, 1380, 1630 and 2210 nm. They have 1000m IFOV except for 250m in 1630nm channel. In our research plan, CLAUDIA (Ishida et al. 2009) algorithm will use channels of 670nm (VN8), 865nm (VN11), 1380nm (SW2), 1630nm (SW3), 10.8 $\mu\text{m}$  (T1), and 12.0 (T2), the Comprehensive Analysis Program for Cloud Optical Measurement (CAPCOM)

(Nakajima and Nakajima 1995, Kawamoto et al. 2001) will use mainly 1050nm (SW1), 1630nm (SW3), and 2210nm (SW4) but optionally use 670nm (VN8) and 865nm (VN10) as well.

## 2. RETRIEVALS OF CLOUD AND AEROSOLS

### 2.1 Cloud and clear discrimination

One of the products from SGLI observation is the Clear Confidence Level (CCL), which is a kind of cloud flag for quantitative representation of clear or cloudy condition. The CCL is derived with the algorithm CLAUDIA. In general, cloud flag algorithms tend to have bias to cloudy or clear. For example, the algorithm used for operational analyses of MODIS data (MOD35, MYD35) biases to cloudy, because MOD35 and/or MYD35 are designed to avoid cloudy pixels as much as possible for reliable extraction of clear-sky areas: this design concept is referred to as “clear conservative”, whereas algorithms that bias to clear are referred to as “cloud conservative”. However, if the cloud flag from an algorithm with clear conservative are used for retrieval of cloud properties, clear-sky pixels are likely to be contaminated. On the other hand, algorithms with cloud conservative reduce areas to retrieve cloud properties. Therefore, we need to use a neutral cloud flag algorithm.

The CLAUDIA uses threshold tests that can be categorized into two groups. Threshold tests in the group 1 are sensitive for cloud areas but tend to incorrectly identify clear areas as cloudy due to confusing ground surface. On the other hand, threshold tests in the group 2 can correctly extract cloudy areas, but tend to incorrectly identify cloudy areas as clear. Threshold tests with thermal infrared radiation tend to be categorized into group 2. Considering the categorization of threshold tests, CLAUDIA derives the overall CCL from results of each test with ensuring neutral cloud screening. The representative value of the CCL for group 1,  $G_1$ , is derived from the geometric mean as follows,

$$G_1 = 1 - \sqrt[n]{(1 - F_1) \cdot (1 - F_2) \cdots (1 - F_k) \cdots (1 - F_n)}, \quad (1)$$

where  $F_k$  is CCL of the  $k$ -th threshold test, and  $n$  is the number of threshold tests in group 1. Eq.2-1 means that when CCLs of all tests in are 0,  $G_1$  is 0 (cloudy), whereas even if only one test is 1,  $G_1$  is 1 (clear). On the other hand, the representative value for group 2,  $G_2$ , is determined from Eq. (2);

$$G_2 = \sqrt[m]{F_1 \cdots F_k \cdots F_m}, \quad (2)$$

where  $m$  is the number of threshold tests in group 2, which means that when CCLs of all tests in are 1,  $G_2$  is 1 (clear), whereas even if only one test is 0,  $G_2$  is 0 (cloudy). This implies that the representative value of group 1 is derived to be “cloud conservative” and that of group 2 is derived to be “clear conservative”. Finally, overall CCL ( $Q$ ) is derived from Eq. (3);

$$Q = \sqrt[3]{G_1 G_2}, \quad (3)$$

which implies that the cloud discrimination of group 2 has priority. Figure 1 is the overall CCL for the MODIS data, as an example of CLAUDIA results. Comparison of the result to the RGB image (Fig. 1(a)) proves that the cloud screening result is almost correct, both over desert and forest. Thin clouds and merges of thick clouds tend to have overall CCL of between 0 and 1, which suggests that CLAUDIA can extract ambiguous areas, with resulting in neutral cloud screening. Moreover, we are going to compare CCL obtained from CLAUDIA with cloud masks obtained from combined use of the Lidar and Radar (Okamoto et al. 2007, 2008, Hagihara et al. 2010) in order to understand characteristics of CLAUDIA performance.

### 2.2 Cloud optical and microphysical properties

The CAPCOM uses LUT (Look up Table)-Iteration Method (LIM) to retrieve the cloud optical and microphysical properties from satellite-derived radiance data. In the CAPCOM, a non-absorption band, an absorption band, and a thermal band, are used to derive cloud optical thickness (CLOP), cloud effective particle radius (CLER), and cloud top temperature (CLTT). Adding to these radiance data, some ancillary input data, such as the vertical profile of the temperature, pressure, water vapor, ground albedo are also used to calculate related geophysical parameters; cloud top height (CLHT) and cloud top pressure (CLTP) are retrieved by comparing cloud top temperature and temperature profile from ancillary data; liquid water path (CLWP) is calculated by cloud optical thickness and effective particle radius. The difference between former CAPCOM (ATSK3R algorithm in the GLI mission) is that the SGLI version will use 1.6- $\mu\text{m}$  and 2.2- $\mu\text{m}$  bands whereas 3.7- $\mu\text{m}$  in the ATSK1. It allows more simple iteration process because no thermal emission components are included in 1.6- $\mu\text{m}$  and 2.2- $\mu\text{m}$  bands. Figure 2 illustrates a tentative flow chart of the CAPCOM optimized to the SGLI specifications. During the

next tree year's period, we will optimize the CAPCOM with to the SGLI specifications. This includes preparation of the LUTs used in the CAPCOM.

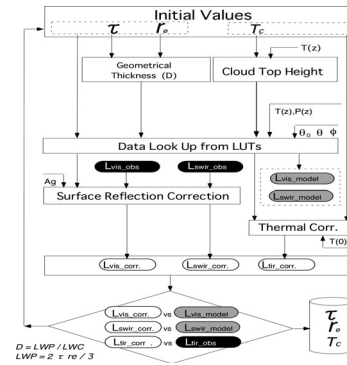


Fig. 2 Flow chart of the CAPCOM.

### 2.3 Cloud geometrical thickness

Reflectance of the 0.763- $\mu\text{m}$  oxygen-A branch has cloud geometrical information such as cloud top height or cloud geometrical thickness (Kuji and Nakajima 2006). It is our one of challenges to retrieve, optical, microphysical, and geometrical properties for clouds from the SGLI. Figure 3 illustrates tentatively retrieved cloud parameters.  $\tau_c$ ,  $r_e$ , LWP,  $Z_t$ ,  $\Delta Z$ ,  $Z_b$  denote cloud optical thickness, effective particle radius, Liquid Water Path, Cloud top height, cloud geometrical thickness, and cloud bottom height. Midori-II/GLI data on 20 March 2003 was used. During the SGLI era, we will improve algorithm and validate these parameters by use of e.g. radar and/or lidar instruments aboard the CloudSat, CALIPSO, and EarthCARE.

### 2.4 Aerosol properties

Retrieving aerosol properties is important to understand aerosol-cloud interactions. The SGLI has many channels for this objective. We are going to retrieve aerosol optical thickness (AOT), size information (Ångström exponent) and single scattering albedo ( $\omega_0$ ) by the combined use of 0.38-, and 0.41- $\mu\text{m}$  reflectances and polarization of 0.67- and 0.87- $\mu\text{m}$  channels (Sano et al., 2009). Figure 4 shows retrieved AOT, Angstrom exponents, and aerosol index. Retrieved results will validate with world wide deployed sun/sky radiometer network (AERONET) data.

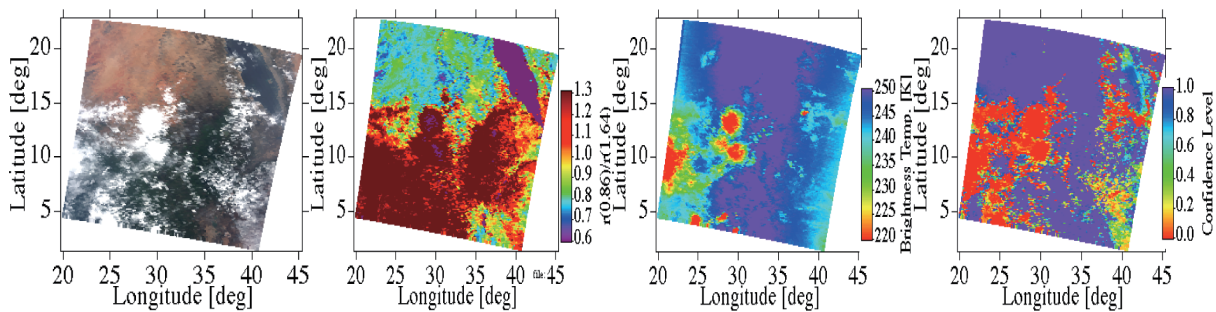


Fig. 1 An example of threshold tests: (a) RGB composite image, (b) the ratio of reflectance of 0.87 $\mu\text{m}$  to 1.64 $\mu\text{m}$ , (c) brightness temperature of 13.9 $\mu\text{m}$ . (d) Overall CCL for the Terra/MODIS derived form CLAUDIA. Data are obtained from Terra/MODIS (over Saharan desert at 2006 Jul. 18).

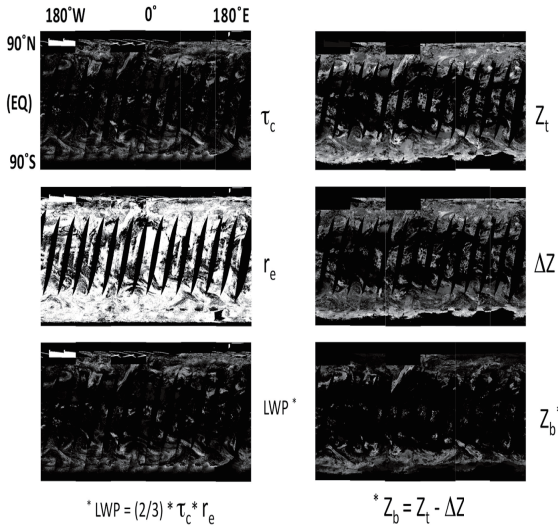


Fig. 3 Tentatively retrieved cloud parameters,  $\tau_c, r_e, LWP, Z_t, \Delta Z, Z_b$  denote cloud optical thickness, effective particle radius, Liquid Water Path, Cloud top height, cloud geometrical thickness, and cloud bottom height. Midori-II/GLI data on 20 Mar, 2003.

### 3. WHAT'S NEW IN GCOM-C ERA

#### 3.1 Collaboration with models

The cloud properties retrieved from the satellite remote sensing described above are further compared with cloud microphysics model to obtain a physical insight into the statistical behavior of the satellite-observed cloud parameters. For this purpose, we will use a non-hydrostatic spectral bin microphysics cloud model (Suzuki et al., 2005), which represents the cloud particle growth processes through the explicit prediction of size distribution functions due to the microphysical processes including nucleation from aerosol, condensation and collision-coagulation processes as schematically shown in Fig.5.

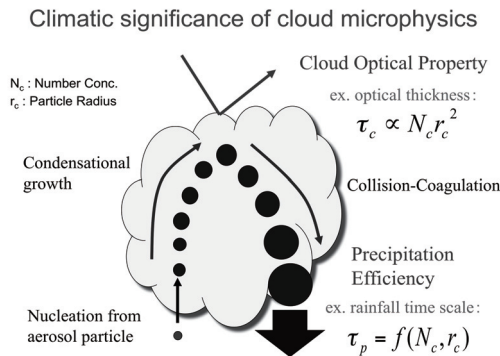


Fig. 5 Schematic viewgraph of cloud growth

The numerical simulations will be performed with this cloud model under the atmospheric conditions that characterize several regions selected across the globe. The results will be compared with satellite remote sensing in terms of the correlation statistics between effective particle radius and

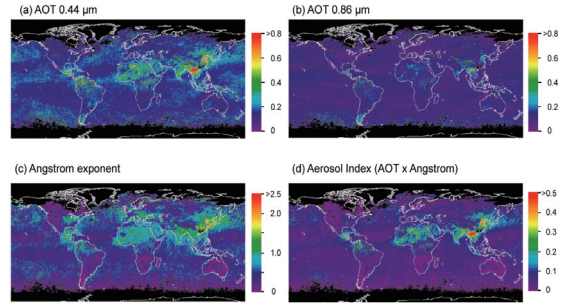


Fig. 4 Global average of the aerosol optical thickness @0.44 $\mu\text{m}$  (a), @0.86 $\mu\text{m}$ , Angstrom exponent (c), and aerosol index (d).

optical thickness of warm clouds. Since the positive and negative correlation patterns between these two quantities are shown to be associated with condensation and coagulation growth processes, respectively, this comparison will provide a physical interpretation of how the cloud microphysical processes are involved in the statistical features of the retrieved cloud parameters. The model results will also be employed to explore how the cloud vertical structures influence the retrieval results of cloud properties especially for effective particle radius. This comparison would provide better quantitative estimates of possible errors that satellite remote sensing suffer from.

#### 3.2 Aerosol assimilation

We are developing a global aerosol assimilation system, based on an ensemble Kalman filter (Schutgens et al. 2010a, 2010b) (Fig. 6 and 7). An ensemble of aerosol transport model calculations for different emission scenarios will be compared to AOT and Ångström exponent observations from SGLI and other sensor (networks) and yield improved global estimates of aerosol bulk scattering properties, loads and forcings. The Kalman filter is an optimal methodology to combine disparate observations and model simulations into a comprehensive picture of the aerosol system. By modifying the filter into a Kalman smoother, we can also hope to obtain better estimates of current aerosol emissions.

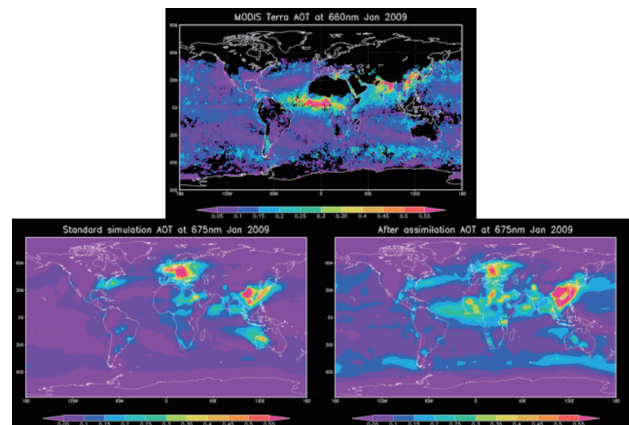


Fig. 6 Monthly averaged AOT for January 2009 from MODIS Terra, the standard SPRINTARS simulation and the simulation with ensemble Kalman filter.

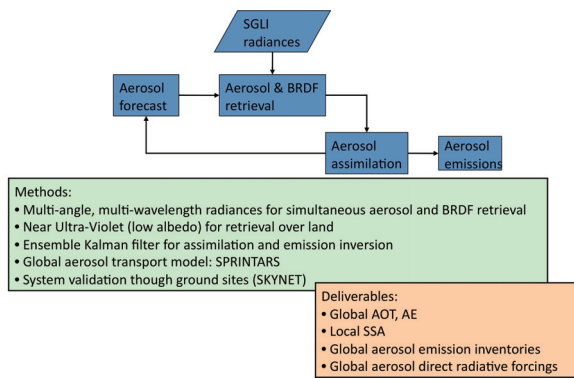


Fig. 7 Flow chart of the aerosol data assimilation

### Acknowledgement

This work was supported by Global Change Observation Mission – Climate (GCOM-C) (2009-2010) and the Earth Cloud, the Aerosol Radiation Explorer (EarthCARE) Science Project (2007-2010) of the Japan Aerospace Exploration Agency (JAXA), the Greenhouse Gases Observing Satellite (GOSAT) Science Project of the National Institute of Environmental Studies (NIES), Tsukuba, Japan (2006-2010).

### References

- Ackerman, S. A., K. I. Strabala, W. P. Menzel, R. A. Frey, C. C. Moeller, and L. E. Gumley, 1998: Discriminating Clear-sky from Clouds with MODIS. *J. Geophys. Res.*, **103**, 32,141-132,157.
- Hagihara, Y., H. Okamoto, and R. Yoshida, 2010: Development of a combined CloudSat/CALIPSO cloud mask to show global cloud distribution. *J. Geophys. Res.*, doi:10.1029/2009JD012344, in press.
- Higurashi, A., T. Nakajima, B. N. Holben, A. Smirnov, R. Frouin, and B. Chatenet, 2000: A study of global aerosol optical climatology with two-channel AVHRR remote sensing. *Journal of Climate*, **13**, 2011-2027.
- Ishida, H., and T. Y. Nakajima, 2009: Development of an unbiased cloud detection algorithm for a spaceborne multispectral imager. *Journal of Geophysical Research-Atmospheres*, doi:10.1029/2008JD010710.
- Kuji, M. and T. Nakajima, 2006: Retrieval of cloud geometrical properties using ADEOS-II/GLI data for radiation budget studies. *SPIE, Remote Sensing of Clouds and the Atmosphere X*, Klaus Schäfer, Adolfo Comerón, James R. Slusser, Richard H. Picard, Michel R. Carleer, Nicolaos Sifakis, Editors, October 2005, 64080
- Mano, Y., 2000: Exact solution of electromagnetic scattering by a three-dimensional hexagonal ice column obtained with the boundary-element method. *Applied Optics*, **39**, 5541-5546.
- Nakajima, T. Y., T. Nakajima, A. Kokhanovsky, 1997: Radiative transfer through light-scattering media with nonspherical large particles: direct and inverse problems. *SPIE, Satellite Remote Sensing of Clouds and the Atmosphere II*, edited by Joanna D. Haigh, *Proceedings of SPIE Vol. 3220 (SPIE, Bellingham, WA 1997)* pp. 2-12.
- Nakajima, T. Y., A. Higurashi, T. Nakajima, S. Fukuda, and S. Katagiri, 2009a: Development of the cloud and aerosol retrieval algorithms for ADEOS-II/GLI mission. *Journal of Remote Sensing Society of Japan*, **29**, 60-69.
- Nakajima, T. Y., T. Nakajima, K. Yoshimori, S. K. Mishra, and S. N. Tripathi, 2009b: Development of a light scattering solver applicable to particles of arbitrary shape on the basis of the surface integral equations method of Müller-type (SIEM/M): Part I. Methodology, accuracy of calculation, and electromagnetic current on the particle surface. *Applied Optics*, **48**, 3526–3536.
- Okamoto, H., T. Nishizawa, T. Takemura, H. Kumagai, H. Kuroiwa, N. Sugimoto, I. Matsui, A. Shimizu, A. Kamei, S. Emori, and T. Nakajima, 2007: Vertical cloud structure observed from shipborne radar and lidar, mid-latitude case study during the MR01/K02 cruise of the R/V Mirai, *J. Geophys. Res.*, **112**, D08216, doi:10.1029/2006JD007628,
- Okamoto, H., T. Nishizawa, T. Takemura, K. Sato, H. Kumagai, Y. Ohno, N. Sugimoto, A. Shimizu, I. Matsui, and T. Nakajima, 2008: Vertical cloud properties in the tropical western Pacific Ocean: Validation of the CCSR/NIES/FRCGC GCM by shipborne radar and lidar, *J. Geophys. Res.*, **113**, D24213, doi:10.1029/2008JD009812.
- Sano, I., Y. Okada, M. Mukai, and S. Mukai, 2009: Retrieval algorithm based on combined use of POLDER and GLI data for biomass aerosols. *J. Rem. Sens. Soc. Jpn*, **29**(1), 54–59.
- Schutgens N.A.J., T. Miyoshi, T. Takemura, T. Nakajima, 2010: Sensitivity tests for an ensemble Kalman filter for aerosol assimilation, submitted to *ACP*.
- Schutgens N.A.J., T. Miyoshi, T. Takemura, T. Nakajima, 2010: Applying an ensemble Kalman filter to the assimilation of AERONET observations in a global aerosol transport model, *ACP*, **10**, 2561 – 2576.
- Solomon, S., 2007: IPCC (Intergovernmental Panel on Climate Change) (2007), *Climate Change 2007: The Physical Science Basis*. Cambridge Univ. Press, Cambridge, UK and New York, USA., 996 pp.
- Suzuki, K., T. Nakajima, T. Y. Nakajima, and A. P. Khain, 2010: A study of microphysical mechanisms for correlation patterns between droplet radius and optical thickness of warm clouds with a spectral bin microphysics cloud model. *J. Atmos. Sci.*, **67**, 1126-1141.
- Suzuki, K., T. Nakajima, T. Y. Nakajima, and A. Khain, 2006: Correlation Pattern between Effective Radius and Optical Thickness of Water Clouds Simulated by a Spectral Bin Microphysics Cloud Model. *SOLA*, **2**, 116-119.